

## High spin levels populated in multinucleon-transfer reactions with 480 MeV $^{12}\text{C}$

L. Kraus, A. Boucenna, I. Linck, B. Lott, R. Rebmeister, N. Schulz, and J. C. Sens  
*Centre de Recherches Nucléaires et Université Louis Pasteur, F-67037 Strasbourg Cedex, France*

M. C. Mermaz, B. Berthier, R. Lucas, J. Gastebois, A. Gillibert,  
A. Miczaika, and E. Tomasi-Gustafsson  
*Département de Physique Nucléaire, Centre d'Etudes Nucléaires de Saclay, F-91191 Gif-sur-Yvette Cedex, France*

C. Grunberg

*Grand Accélérateur National à Ions Lourds (GANIL), F-14021 Caen Cedex, France*

(Received 24 February 1988)

Two- and three-nucleon stripping reactions induced by 480 MeV  $^{12}\text{C}$  have been studied on  $^{12}\text{C}$ ,  $^{16}\text{O}$ ,  $^{28}\text{Si}$ ,  $^{40}\text{Ca}$ , and  $^{54}\text{Fe}$  target nuclei. Discrete levels are fed with cross sections up to 1 mb/sr for d-transfer reactions and 1 order and 2 orders of magnitude less for 2p- and  $^3\text{He}$ -transfer reactions, respectively. These reactions preferentially populate high spin states with stretched configurations. Several spin assignments were known from transfer reactions induced by lighter projectiles at incident energies well above the Coulomb barrier. In the case of two-nucleon transfer reactions, the energy of these states is well reproduced by crude shell model calculations. Such estimates are of use in proposing spins of newly observed states especially as the shapes of the measured angular distributions are independent of the final spin of the residual nucleus.

### I. INTRODUCTION

It is well known that multinucleon stripping reactions induced by heavy ions of high incident energies will preferentially populate high spin states. This selectivity, which allows spectroscopic studies, was already established in the work of Anyas-Weiss *et al.*<sup>1</sup> and of Homeyer *et al.*<sup>2</sup> for 1p shell projectiles bombarding target nuclei of the 1p, 2s-1d, and 1f-2p shells well above the Coulomb barrier. It is also encountered in the ( $\alpha$ ,d) and ( $\alpha$ , $^2\text{He}$ ) reactions (see Refs. 3 and 4, 5, respectively). For few-nucleon transfer reactions the relevant selectivity is due, on the one hand, to the large orbital angular momentum mismatch between the grazing waves in the entrance and exit channels which favors a large transfer of angular momentum, and on the other hand, to large 0s cluster spectroscopic factors expected theoretically for final high spin states with stretched configurations. The energies of these high spin states can be successfully predicted by a crude shell model estimate in the case of two-nucleon-transfer reactions as has been shown by Tsan Ung Chan.<sup>6</sup>

In this paper we shall present the results concerning the two-proton-, deuteron-, and  $^3\text{He}$ -stripping reactions induced by 480 MeV  $^{12}\text{C}$ . The position of the high spin states will be compared with the crude shell model predictions and the angular distributions of the most strongly populated states will be analyzed in the framework of the exact finite range distorted waves Born approximation (EFR-DWBA) using the 0s cluster approximation. The target nuclei were  $^{12}\text{C}$ ,  $^{16}\text{O}$ ,  $^{28}\text{Si}$ ,  $^{40}\text{Ca}$ , and  $^{54}\text{Fe}$ . We were able to confirm, and in some cases to propose, spins and configurations for highly excited levels.

### II. EXPERIMENTAL ARRANGEMENT

The multinucleon transfer reactions on light and medium weight target nuclei were performed at the Grand Accélérateur National à Ions Lourds (GANIL) facility using the 480 MeV  $^{12}\text{C}$  beam. The  $^{10}\text{Be}$ ,  $^{10}\text{B}$ , and  $^9\text{Be}$  ejectiles were momentum analyzed and identified using the energy loss magnetic spectrometer<sup>7</sup> SPEG and its associated equipment. The detection system consisted of (i) two ( $x,y$ ) position sensitive drift chambers having a spatial resolution of 0.6 mm in each direction, located on either side of the focal surface for determining the scattering angle and the magnetic rigidity of the detected particles; (ii) an ionization chamber for measuring the energy loss of the outgoing particles, necessary for their identification; and (iii) two plastic scintillators, one providing the start signal for the time of flight and the other serving as a veto counter for the rejection of light particles. The rf of the second GANIL cyclotron provided the stop signal of the time of flight. All the gas counters were filled with isobutane. With this arrangement, the measured energy resolution was about 200 keV, corresponding to a momentum resolution  $\Delta p/p = 2 \cdot 10^{-4}$ . The total angular aperture in the reaction plane of the spectrometer was  $4^\circ$  in the laboratory frame and the angular distributions were measured in this angular range. The beam emittance for all runs was never larger than  $2\pi$  mm mrad, which permitted an angular binning of  $0.5^\circ$  in the angular distributions. The absolute values for all reaction cross sections were obtained from the target thickness measured with the alpha gage technique and from the beam current monitor. These absolute values are uncertain by a factor of 2 mainly because of uncertainties in



Inserting these approximations into Eq. (2) gives the shell model formula proposed by Tsan Ung Chan,<sup>6</sup>

$$E^*(A_0 + 2N, j_1 j_2 JT) = 2E_B(A_0 + N, \text{g.s.}) - E_B(A_0, \text{g.s.}) - E_B(A_0 + 2N, \text{g.s.}) + E^*(A_0 + N, j_1) + E^*(A_0 + N, j_2),$$

in the p-p and n-n cases and

$$E^*(A_0 + N + N', j_1 j_2 JT) = E^*(A_0 + N, j_1) + E^*(A_0 + N', j_2) \quad (3)$$

in the n-p case.

The validity of this model has been checked<sup>6</sup> and confirmed in the present work for known states, thus lending confidence in its use for proposing spins for several unassigned states. Also, comparison for a given two-nucleon configuration of a given experimental excitation energy with this shell model estimation permits extraction of experimental TBME and Coulomb energies which can be compared to calculated ones.

### 2. Three-particle states

Using Eq. (1) for the particular case of the transfer of two protons and one neutron moving with the maximum alignment in the same orbit,  $d_{5/2}$  for instance, we calculate the excitation energy of the final state to be

$$\begin{aligned} E^*(A_0 + 2p + 1n, (\pi d_{5/2})_4^+ \nu d_{5/2}, 13/2^+ 1/2) \\ = E_B(A_0, \text{g.s.}) - E_B(A_0 + 2p + 1n, \text{g.s.}) + 2\varepsilon(\pi d_{5/2}) \\ + \varepsilon(\nu d_{5/2}) + E_C + 1.5 \langle d_{5/2}^2 | V | d_{5/2}^2 \rangle_{4^+, 1} \\ + 1.5 \langle d_{5/2}^2 | V | d_{5/2}^2 \rangle_{5^+, 0}, \end{aligned} \quad (4)$$

where the TBME are deduced from experimental two-particle data. Similar relations can be derived for other configurations.

### B. EFR-DWBA calculations

In multinucleon stripping reactions, high spins are favored for the following reasons:<sup>10</sup> (i) The large orbital angular momentum mismatch between entrance and exit channel grazing waves, due to the large mass of the transferred cluster, favors large  $L_T$ ; furthermore, this transferred angular momentum  $L_T$  increases with the incident energy; and (ii) in the residual nucleus, for high spin states the two-nucleon relative motion wave function has a strong overlap with the  $0s$  cluster wave function which is the one most favored in direct surface transfer reactions. In other words, large  $0s$  spectroscopic factors are expected for these high spin states.

The EFR-DWBA calculations of the angular distributions of multinucleon transfer reactions were performed with the code PTOLEMY (Ref. 11) using the  $0s$  cluster approximation. In this approximation, the  $2N + L$  total number of quanta, where  $N$  is the number of nodes of the radial wave function for the center of momentum (c.m.) motion of the transferred cluster and  $L$  the transferred angular momentum, is equal to the sum of the  $2n + l$  number of quanta for each nucleon in the cluster, accord-

ing to the shell model picture. For unbound cluster states, the EFR-DWBA calculations were performed using the experimental  $Q$  values of the reactions, which is the usual procedure for the computation of the projectile and ejectile distorted waves. The cluster wave functions of the EFR-DWBA kernel integral have been arbitrarily bound by 100 keV.

## IV. RESULTS AND DISCUSSION

### A. Two-proton stripping reactions

In the hypothesis of a  $0s$  diproton transfer on  $0^+$  target nuclei, only natural parity states can be populated. Cross sections are in the range 0.01 to 0.1 mb/sr for the most strongly excited states and decrease as the mass of the target increases.

#### 1. $^{12}\text{C}(^{12}\text{C}, ^{10}\text{Be})^{14}\text{O}$

Figure 1 presents the  $^{12}\text{C}(^{12}\text{C}, ^{10}\text{Be})^{14}\text{O}$  two-proton stripping spectrum at 480 MeV incident energy. The strong population of the 6.27 MeV  $3^-$  and 9.90 MeV  $4^+$  states was already observed in the same reaction at 114 MeV.<sup>1</sup> Furthermore, these two levels, or their analog states, are also strongly populated in the  $^{12}\text{C}(^{11}\text{B}, ^9\text{Li})^{14}\text{O}$  and  $^{12}\text{C}(^{12}\text{C}, ^{10}\text{C})^{14}\text{C}$  reactions<sup>1</sup> for the same incident energy. These two high spin states are the only ones encountered in the  $^{12}\text{C}(^{10}\text{B}, ^8\text{Li})^{14}\text{O}$  two-proton stripping

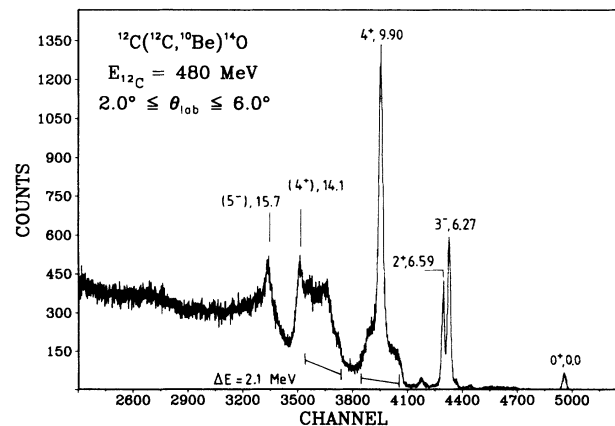


FIG. 1. The  $^{12}\text{C}(^{12}\text{C}, ^{10}\text{Be})^{14}\text{O}$  stripping reaction. The energy resolution (full width at half maximum) is 200 keV. Limits of the Doppler broadening  $\Delta E$  are indicated at the base of two of the peaks.

spectrum with 100 MeV  $^{10}\text{B}$  (Ref. 12). In this work, the analogous  $^{12}\text{C}(^{10}\text{B}, ^8\text{B})^{14}\text{C}$  two-neutron stripping reaction populates only and strongly the 6.72 MeV  $3^-$  and the 10.74 MeV  $4^+$  states in  $^{14}\text{C}$ , as is the case for the  $^{12}\text{C}(\alpha, ^2\text{He})^{14}\text{C}$  stripping at 65 MeV  $\alpha$  energy.<sup>4,5</sup> The two-proton configurations assigned to the 6.27 MeV  $3^-$  and 9.90 MeV  $4^+$  states in the  $^{14}\text{O}$  nucleus,  $(1p_{1/2}1d_{5/2})_{3^-}$  and  $(1d_{5/2})_{4^+}^2$ , respectively, are predicted by the shell model Eq. (3) to lie at 6.23 and 9.78 MeV.

In Fig. 1, a  $2^+$  state located at 6.59 MeV in  $^{14}\text{O}$  is excited almost as strongly as the  $3^-$  level. This is surprising since, as mentioned above, this level has not been observed at lower heavy ion incident energies in experiments of approximately the same resolution as the present one.<sup>1,13</sup> No simple two-particle configuration for this level will fit the angular distribution of the  $^{12}\text{C}(^3\text{He}, n)^{14}\text{O}$  reaction at 25.4 MeV incident energy. Furthermore, the analyzing power angular distribution of this level in the  $^{16}\text{O}(p, t)^{14}\text{O}$  reaction cannot be fitted by DWBA calculations (see Ref. 14 and references therein). A weak coupling calculation performed by Lie<sup>15</sup> for  $A=14$  nuclei predicts a main two-hole configuration with respect to a closed  $1p$  shell for the first  $2^+$ ,  $T=1$  state. This  $(1p)_{2^+}^{-2}$  configuration, implying at least one hole in the target core, cannot be reached by a direct transfer reaction. So the strong excitation of this state in the present experiment results from a mechanism more complex than a direct transfer, bringing into play the high incident energy and possibly smaller components of the  $2^+$  state wave function such as the  $2p$ - $1f$  shell component suggested by an angular correlation measurement.<sup>16</sup>

In the spectrum of Fig. 1, large bumps due to the  $\gamma$ -ray decay in flight of the  $^{10}\text{Be}$  ejectile core excited in its first  $2^+$  state at 3.37 MeV can be seen. The full width  $\Delta E$  at the base of such bumps is equal to  $2E_\gamma V_e/c$ , where  $E_\gamma$  is the excitation energy of the first  $2^+$  state in  $^{10}\text{Be}$ ,  $V_e$  is the speed of the ejectile in the laboratory frame, and  $c$  the velocity of light. This simple relationship is just the usual Doppler broadening formula. In Fig. 1, the bump situated beneath the 9.90 MeV  $4^+$  state is built on the 6.27 MeV  $3^-$  state, while the other bump located around 13.3 MeV is built on the 9.90 MeV  $4^+$  state.

At higher excitation energy, two peaks show up at 14.1 and 15.7 MeV in Fig. 1. Spin-parity assignments to these levels are not straightforward. The only natural parity stretched configuration energetically possible appears to be  $(1d_{5/2}1d_{3/2})_{4^+}$  predicted at 14.23 MeV. Other high spin configurations need a contribution of the  $f_{7/2}$  shell. Since the first  $7/2^-$  state in  $^{13}\text{N}$ , located at 10.36 MeV, has a very weak proton spectroscopic factor,<sup>17</sup> the configurations  $(1p_{1/2}1f_{7/2})_{4^+}$ ,  $(2s_{1/2}1f_{7/2})_{3^-}$ , and  $(1d_{5/2}1f_{7/2})_{5^-}$ , predicted with this energy at 13.04, 15.4, and 16.6 MeV, respectively, are unlikely. The same dilemma is encountered<sup>4,5,12</sup> for the 14.9 MeV state of  $^{14}\text{C}$ .

Figure 2 presents the  $^{12}\text{C}(^{12}\text{C}, ^{10}\text{Be})^{14}\text{O}$  angular distributions measured at 480 MeV  $^{12}\text{C}$  fitted by the EFR-DWBA calculations. The agreement in shape is very good. However, the shapes have no spin dependence.

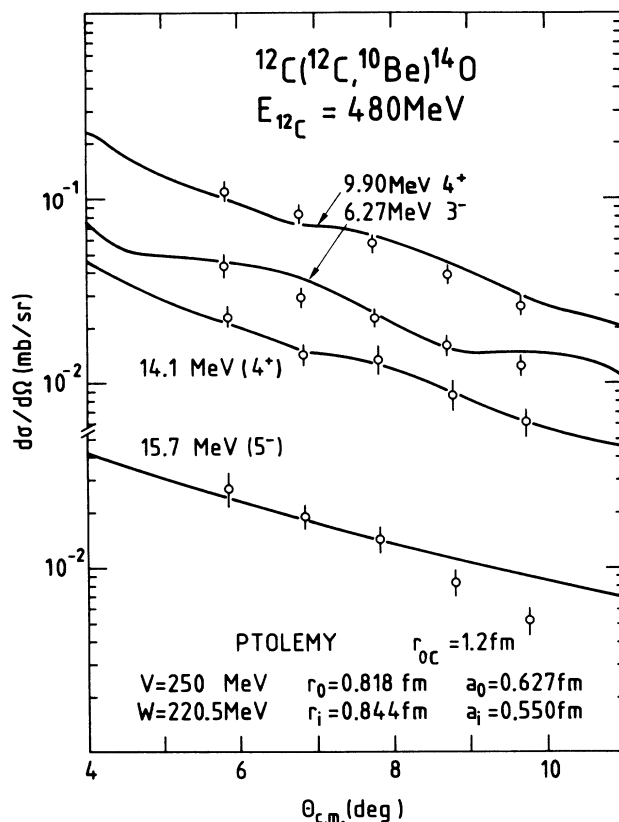


FIG. 2. Angular distributions of the  $^{12}\text{C}(^{12}\text{C}, ^{10}\text{Be})^{14}\text{O}$  stripping reaction. The curves are the results of EFR-DWBA calculations using the optical model parameters given in the figure. The normalization factors (experiment/theory) are 0.175, 0.065, 0.016, and 0.005 for the 6.27 MeV  $3^-$ , 9.90 MeV  $4^+$ , 14.1 MeV  $4^+$ , and 15.7 MeV  $5^-$  states, respectively.

The optical model parameters used in the present calculations are given in Fig. 2 and fit best the 420 MeV elastic scattering data of Sahm *et al.*<sup>18</sup> The normalization factors,  $\sigma_{\text{exp}}/\sigma_{\text{DWBA}}$ , are reported in the figure caption.

## 2. $^{16}\text{O}(^{12}\text{C}, ^{10}\text{Be})^{18}\text{Ne}$

Figure 3 presents the two-proton stripping spectrum obtained with 480 MeV  $^{12}\text{C}$  on a  $\text{SiO}_2$  target. The different angular kinematic shifts of the reaction products, arising either from a reaction on  $^{16}\text{O}$  or on  $^{28}\text{Si}$ , allow one to partly disentangle the two reactions. The broad peaks of Fig. 3 are due to the fact that in the data reduction procedure, the position of the focal surface is reconstructed for the  $^{28}\text{Si}$  target and not for  $^{16}\text{O}$ . This effect is particularly visible for the  $^{18}\text{Ne}$ , 3.4 MeV,  $4^+$  level which exhibits a large width. We shall discuss first the  $^{16}\text{O}(^{12}\text{C}, ^{10}\text{Be})^{18}\text{Ne}$  two-proton stripping reaction.

The 3.38 MeV  $4^+$  state of the  $^{18}\text{Ne}$  nucleus is already strongly excited in the  $^{16}\text{O}(^{10}\text{B}, ^8\text{Li})^{18}\text{Ne}$  reaction;<sup>12</sup> so is the 3.55 state of the analog  $^{18}\text{O}$  nucleus in the  $^{16}\text{O}(^{10}\text{B}, ^8\text{B})^{18}\text{O}$  (Ref. 12) and  $^{16}\text{O}(\alpha, ^2\text{He})^{18}\text{O}$  (Ref. 4) reactions. A  $(1d_{5/2})_{4^+}^2$  configuration is predicted by Eq. (3) at 3.32 MeV excitation. At higher energy, the level ob-

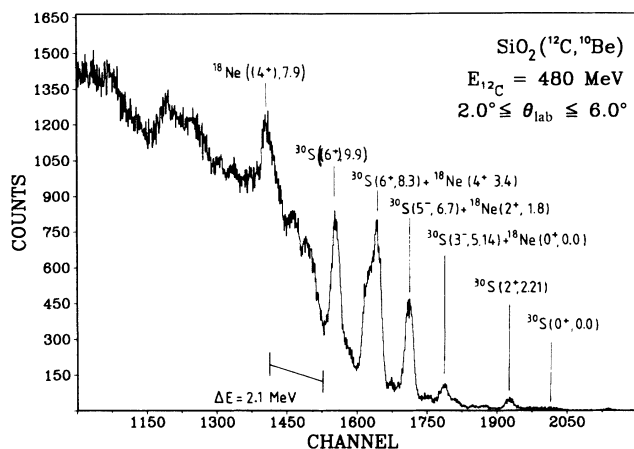


FIG. 3. The spectrum of the  $(^{12}\text{C}, ^{10}\text{Be})$  stripping reaction on a  $\text{SiO}_2$  target. The indicated limits of the Doppler broadening  $\Delta E$  are for the exit channel  $^{30}\text{S}^*(6.7) + ^{10}\text{Be}^*(3.37)$ .

served at 7.9 MeV could possibly have the stretched  $(1d_{5/2}1d_{3/2})_{4+}$  configuration, calculated at 8.32 MeV. A  $4^+$  level with dominant configuration  $(1d_{5/2}1d_{3/2})$  has recently been identified in  $^{18}\text{O}$  at an excitation energy of 9.0 MeV.<sup>19</sup> This is to be compared with the 8.99 MeV value of the shell model.

### 3. $^{28}\text{Si}(^{12}\text{C}, ^{10}\text{Be})^{30}\text{S}$

We shall consider now the  $^{30}\text{S}$  spectrum populated by the  $(^{12}\text{C}, ^{10}\text{Be})$  two-proton stripping reaction. The 2.21 MeV  $2^+$  level is already well known:<sup>20</sup> its dominant configuration is  $(2s_{1/2}1d_{3/2})_{2+}$ . The 5.14 MeV state, which would correspond (see Fig. 4) to the analog 5.49 MeV  $3^-$  level<sup>20</sup> of  $^{30}\text{Si}$  populated by the  $^{28}\text{Si}(\alpha, ^2\text{He})^{30}\text{Si}$  reaction at 65 MeV,<sup>4,5</sup> is not strongly excited in the present reaction. This is consistent with the proposed<sup>5</sup>  $(2s_{1/2}1f_{7/2})_{3-}$  natural parity configuration which, however, does not correspond to the state predicted by Eq. (3) at 5.10 MeV for the maximum alignment of the valence nucleons. The strongly populated states at 6.7, 8.3, and 9.9 MeV in  $^{30}\text{S}$  would correspond to the 7.04, 8.95, and 10.67 MeV states of  $^{30}\text{Si}$  observed in the  $(\alpha, ^2\text{He})$  reaction.<sup>4,5</sup> The positions of the first two states are indeed in good agreement with the values 6.48 and 8.55 MeV predicted from Eq. (3) for the proposed<sup>4,5</sup> respective configurations  $(1d_{3/2}1f_{7/2})_{5-}$  and  $(1f_{7/2})_{6+}^2$ . The  $J^\pi$  assignment of the 9.9 MeV state could be  $6^+$  since the 10.67 MeV  $^{30}\text{Si}$  state is well established to be  $6^+$  by a DWBA angular distribution fit.<sup>5</sup> However, one has to disregard the proposed<sup>4</sup>  $(1f_{7/2}1f_{5/2})_{6+}$  configuration which was based on a  $5/2^-$  assignment in place of the now established  $7/2^-$  for the 6.19 state of  $^{29}\text{Si}$ .<sup>20</sup> One notices that the energy difference between the second and first  $6^+$  states is of the order of the  $2^+$  state excitation energy of the target nucleus, so the 9.9 MeV state would be produced by a two-proton transfer to the  $f_{7/2}$  subshell on a polarized target core. This hypothesis is strengthened

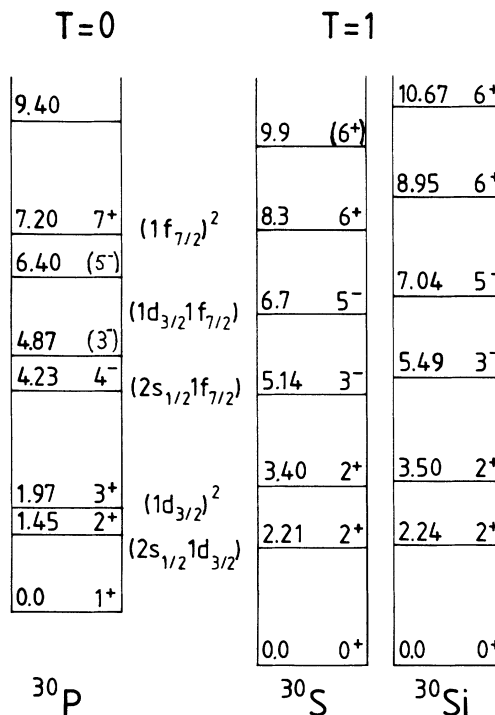


FIG. 4. Levels of  $A=30$  nuclei excited by two-particle transfer reactions in  $^{30}\text{Si}$  (Refs. 4, 5, and 20), in  $^{30}\text{S}$  (Ref. 20 and present work), and in  $^{30}\text{P}$  (Refs. 20, 27, and present work).

by the fact that similar energy differences are observed between the two  $6^+$  states in  $^{30}\text{Si}$  as well as in  $^{34}\text{S}$  (Ref. 4) for target nuclei with strong  $B(E2, 2^+ \rightarrow 0^+)$  values.

Figure 5 presents the angular distributions obtained for two excited levels of  $^{30}\text{S}$ . The EFR-DWBA curves agree well in shape with the experimental data. The optical model parameters used are given in the figure and come from a best elastic scattering fit of 420 MeV  $^{12}\text{C}$  on a  $^{40}\text{Ca}$  target.<sup>18</sup>

### 4. $^{40}\text{Ca}(^{12}\text{C}, ^{10}\text{Be})^{42}\text{Ti}$

Figure 6 presents the spectrum of the  $^{40}\text{Ca}(^{12}\text{C}, ^{10}\text{Be})^{42}\text{Ti}$  two-proton stripping reaction measured at 480 MeV. The known 3.04 MeV  $6^+$  state, having a  $(1f_{7/2})_{6+}^2$  configuration predicted by Eq. (3) at 2.68 MeV, is strongly populated. This state was already observed in the same reaction<sup>1</sup> at the lower incident energy of 114 MeV. Two additional  $^{42}\text{Ti}$  states are present in the spectrum. For the weakly populated 4.4 MeV level, contradictory spin assignments have been proposed:  $2^+$ ,  $4^+$ , and  $3^-$  (see Refs. 21, 22, and 23, respectively). The value  $4^+$  and the weak feeding of this level could be explained by the  $(1f_{7/2}2p_{3/2})_{4+}$  configuration, since the stretched configuration  $(1f_{7/2}2p_{3/2})_{5+}$  is predicted from Eq. (3) at 4.39 MeV excitation. The strong 7.5 MeV peak yield could correspond to a  $6^+$  state with a  $(1f_{7/2}1f_{5/2})_{6+}$  two-proton configuration calculated at 8.39 MeV. The large yield for this state would be expected for a high natural parity spin.

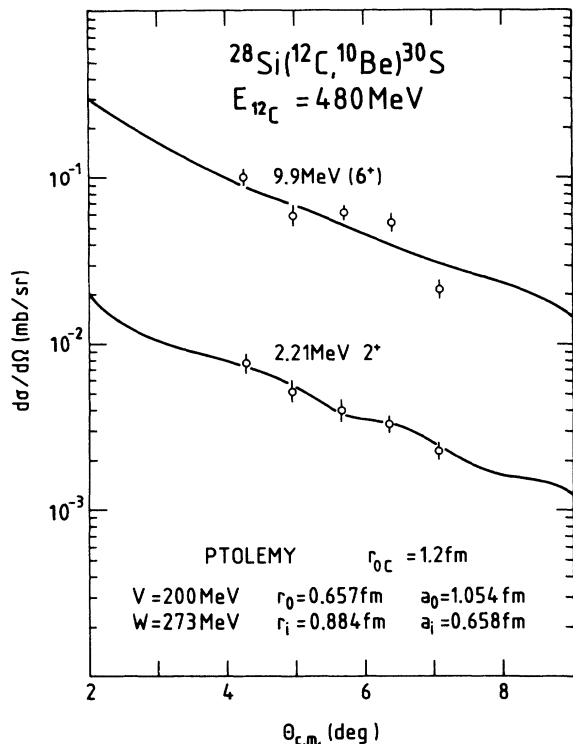


FIG. 5. Angular distributions of the  $^{28}\text{Si}(^{12}\text{C},^{10}\text{Be})^{30}\text{S}$  stripping reaction. The curves are the results of EFR-DWBA calculations, with normalization factors (experiment/theory) 0.67 for the 2.21 MeV  $2^+$  level and 0.07 for the 9.9 MeV ( $6^+$ ) level.

### 5. $^{54}\text{Fe}(^{12}\text{C},^{10}\text{Be})^{56}\text{Ni}$

Figure 7 presents the  $^{54}\text{Fe}(^{12}\text{C},^{10}\text{Be})^{56}\text{Ni}$  two-proton stripping results for 480 MeV. The transitions to the g.s.  $0^+$ , the 2.70 MeV  $2^+$ , the 3.92 MeV  $4^+$ , and the 5.32 MeV  $6^+$  levels were already known, since these states are populated by the same reaction at 78 MeV.<sup>2,24</sup> They were

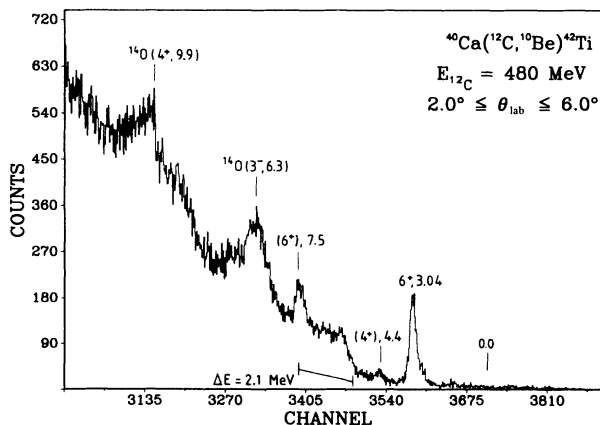


FIG. 6. The  $^{40}\text{Ca}(^{12}\text{C},^{10}\text{Be})^{42}\text{Ti}$  stripping reaction. The target contained carbon as a contaminant. The Doppler broadening corresponds to the exit channel  $^{42}\text{Ti}^*(3.04) + ^{10}\text{Be}^*(3.37)$ .

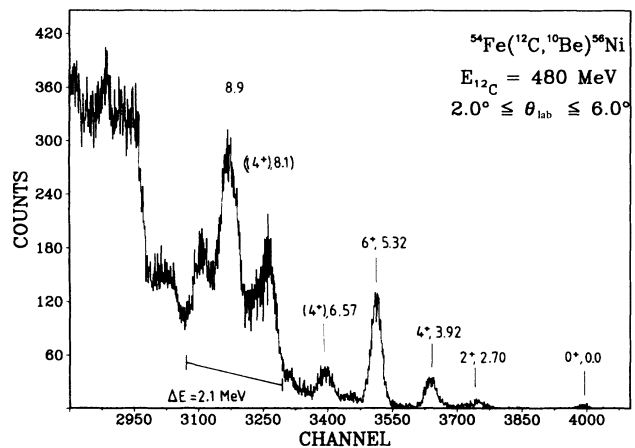


FIG. 7. The  $^{54}\text{Fe}(^{12}\text{C},^{10}\text{Be})^{56}\text{Ni}$  two-proton stripping reaction. The Doppler broadening  $\Delta E$  corresponds to the  $^{56}\text{Ni}^*(5.32) + ^{10}\text{Be}^*(3.37)$  channel.

also observed in the  $^{54}\text{Fe}(^{16}\text{O},^{14}\text{C})^{56}\text{Ni}$  two-proton stripping reaction performed at 104 MeV  $^{16}\text{O}$ .<sup>2,24</sup> From the shell model estimate, the stretched spin configuration  $(1f_{7/2}1f_{5/2})_{6^+}$  predicted at 5.41 MeV, should be attributed to the 5.32 MeV state. A ( $4^+$ ) spin has been proposed<sup>2</sup> for the 6.57 MeV level of  $^{56}\text{Ni}$ . This assignment is supported by the 6.26 MeV excitation calculated for a state having a  $(1f_{7/2}2p_{1/2})_{4^+}$  two-proton configuration. For the 8.1 and 8.9 MeV  $^{56}\text{Ni}$  peaks which are embedded in the bump of the mutual excitation of the ejectile and residual nucleus, only tentative level spins can be assigned on the basis of the crude shell model formula alone. Because of the strong population of these states, we consider only the high spin configurations predicted in this excitation region:  $(2p_{3/2}1f_{5/2})_{4^+}$  at 7.57 MeV,  $(1f_{5/2})_{4^+}^2$  at 8.70 MeV,  $(1f_{7/2}1g_{9/2})_{7^-}$  at 8.17 MeV, and  $(2p_{3/2}1g_{9/2})_{5^-}$  at 10.33 MeV. Note the large width of the 8.9 MeV peak which probably corresponds to a doublet. On the other hand, a DWBA analysis of the  $(^{12}\text{C},^{10}\text{Be})$  and  $(^{16}\text{O},^{14}\text{C})$  data for lower bombarding energies<sup>2</sup> yields  $4^+$ ,  $6^+$ , and  $4^+$  assignments for the observed<sup>2</sup> 8.0, 8.7, and 9.1 MeV states. A  $(1g_{9/2})_{8^+}^2$  configuration has been proposed for two-neutron states populated under 10 MeV excitation energy by  $(\alpha,^2\text{He})$  reactions on  $1f$ - $2p$  shell target nuclei.<sup>25</sup> For the present doubly magic  $^{56}\text{Ni}$ , a state with such a configuration is expected at 14.2 MeV, due to the position of the  $1g_{9/2}^+$  state in  $^{55}\text{Co}$ .<sup>26</sup>

Figure 8 presents the experimental angular distributions along with the EFR-DWBA calculations. The optical model parameters used in the computations are given in the figure; they fit best the  $^{12}\text{C}$  elastic scattering on  $^{40}\text{Ca}$  at 420 MeV.<sup>18</sup>

### B. Deuteron stripping reactions

Figure 9 presents the  $(^{12}\text{C},^{10}\text{B})$  deuteron stripping results obtained from a  $\text{SiO}_2$  target with 480 MeV  $^{12}\text{C}$ . The  $^{10}\text{B}$  reaction products, coming either from a reaction on

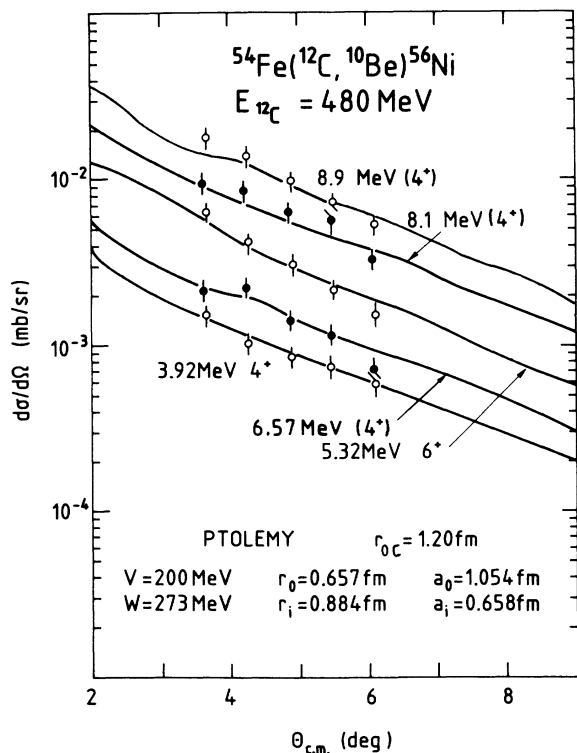


FIG. 8. Angular distributions of the  $^{54}\text{Fe}(^{12}\text{C}, ^{10}\text{Be})^{56}\text{Ni}$  stripping reaction. The fits are the results of EFR-DWBA calculations. The normalization factors (experiment/theory) are 0.007, 0.008, 0.010, 0.041, and 0.074 for the 3.92 MeV  $4^+$ , 5.32 MeV  $6^+$ , 6.57 MeV ( $4^+$ ), 8.1 MeV ( $4^+$ ), and 8.9 MeV ( $4^+$ ), respectively. Other possible assignments for the last state are discussed in the text.

$^{28}\text{Si}$  or  $^{16}\text{O}$ , have been identified by their different kinematic shifts using a bidimensional energy versus angle display. For the spectrum of Fig. 9, the energy resolution was optimized on the  $^{28}\text{Si}$  reaction. Since the spin of the  $^{10}\text{B}$  g.s. is  $3^+$  unnatural parity states can be populated. The n-p pair can be transferred as an  $S=1, T=0$  or an  $S=0, T=1$  cluster. In fact, it has been observed<sup>1</sup> that the cross sections are 10 to 100 times larger for the first case. If the two nucleons are transferred in two different orbits, we give, as the excitation energy of the considered configuration, the mean value obtained by interchanging the proton and neutron in Eq. (3).

### 1. $^{16}\text{O}(^{12}\text{C}, ^{10}\text{B})^{18}\text{F}$

The strongest peak in the spectrum (Fig. 9) corresponds to the 1.12 MeV  $5^+$  level already identified in the same reaction performed<sup>1</sup> at 114 MeV. This level is also strongly populated in  $^{16}\text{O}(\alpha, d)^{18}\text{F}$  on an  $^{16}\text{O}$  gas target at 64.4 MeV.<sup>27</sup> In this ( $\alpha, d$ ) experiment, the deuteron spectrum looks very similar to our  $^{10}\text{B}$  spectrum above 9 MeV excitation in  $^{18}\text{F}$ : the three peaks observed at 9.49, 10.54, and 11.38 MeV in ( $\alpha, d$ ) are located in the present work at 9.35, 10.23, and 11.16 MeV. DWBA fits to deuteron angular distributions led to ( $6^-$ ) and ( $7^+$ ) spin parity assignments for the 9.49 and 10.54 MeV states. Thus a

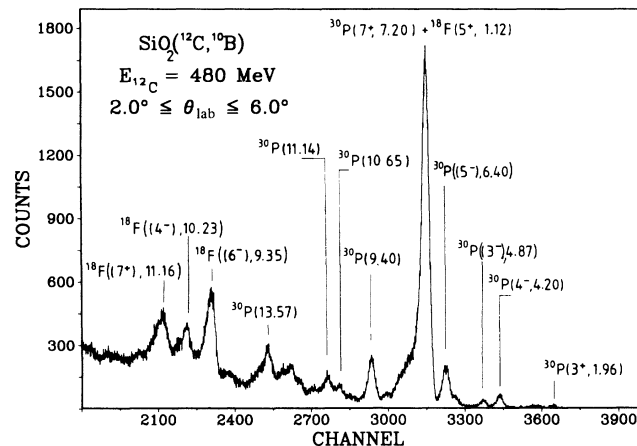


FIG. 9. The energy spectrum of the  $(^{12}\text{C}, ^{10}\text{B})$  deuteron stripping reactions obtained with a  $\text{SiO}_2$  target. Respective contributions of the  $^{18}\text{F}$  (1.12 MeV) and  $^{30}\text{P}$  (7.20 MeV) states have been disentangled by the kinematic shifts.

$(1d_{5/2}1f_{7/2})_{6^-}$  configuration<sup>3,5</sup> and a  $(1f_{7/2})_{7^+}$  configuration<sup>27</sup> have been proposed for these states, respectively. These suggestions rely on an  $f_{7/2}$  single particle energy deduced from the excitation energy of the first  $\frac{7}{2}^-$  level in  $^{17}\text{O}$  and  $^{17}\text{F}$  [roughly 5.7 MeV (Ref. 28)]. But in this mass region, the  $\epsilon(f_{7/2})$  values are usually taken to be of the order of 10 MeV.<sup>29</sup> Such values are in favor of the configuration proposed for the ( $6^-$ ) state and push the  $(f_{7/2})_{7^+}$  two-particle centroid above 20 MeV excitation. According to Eq. (3) and Table I, two stretched p-n configurations are expected in the considered energy region, namely,  $(1d_{3/2})_{3^+}$  at 10.1 MeV and  $(2s_{1/2}1f_{7/2})_{4^-}$  around 10.7 MeV. A possible ( $4^-$ ) state is reported<sup>28</sup> at 10.23 MeV. The stretched p-n configuration  $(1d_{3/2}1f_{7/2})_{5^-}$  should exist around 14 MeV, but was not observed in the present experiment.

Figure 10 presents the angular distributions of the  $^{16}\text{O}(^{12}\text{C}, ^{10}\text{B})^{18}\text{F}$  deuteron stripping reaction. The EFR-DWBA fits are excellent but, unfortunately, independent of the spin of the  $^{18}\text{F}$  final states. The optical model parameters used in these calculations are from Ref. 18, and fit best the  $^{12}\text{C}$  elastic scattering data on  $^{12}\text{C}$  at 420 MeV.

### 2. $^{28}\text{Si}(^{12}\text{C}, ^{10}\text{B})^{30}\text{P}$

Concerning the  $^{28}\text{Si}(^{12}\text{C}, ^{10}\text{B})^{30}\text{P}$  reaction (Fig. 9), several states were already populated in ( $\alpha, d$ ) reaction<sup>27</sup> at 64.4 MeV: 1.97 MeV  $3^+$ , 4.23 MeV  $4^-$ , and 7.23 MeV  $7^+$ . The spin assignments of these states were made on the basis on DWBA fits of the  $^{28}\text{Si}(\alpha, d)^{30}\text{P}$  angular distributions.<sup>27</sup> Fully aligned spin configurations  $(1d_{3/2})_{3^+}$ ,  $(2s_{1/2}1f_{7/2})_{4^-}$ , and  $(1f_{7/2})_{7^+}$  are predicted by Eq. (3) at 2.65, 3.54, and 7.07 MeV, respectively. The 4.87 and 6.40 MeV peaks of the present  $^{30}\text{P}$  data are located in the energy range where the  $(1d_{3/2}1f_{7/2})_{5^-}$  stretched configuration state is expected, as can be seen in Fig. 4.

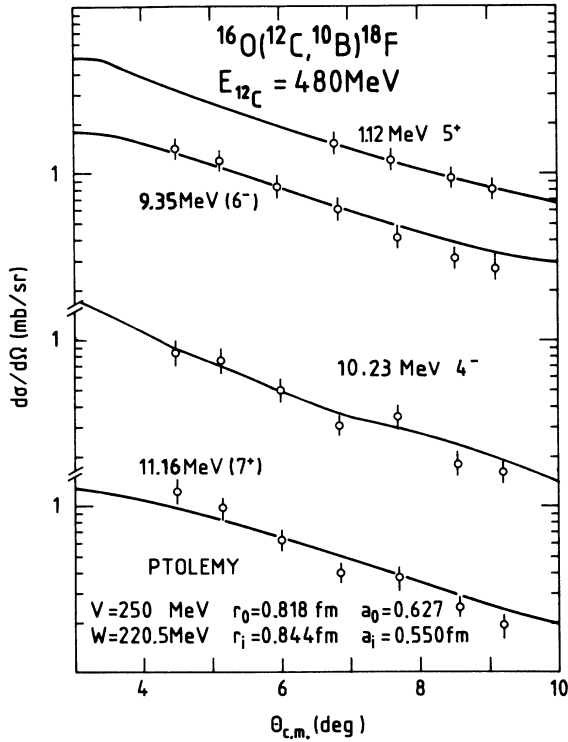


FIG. 10. Angular distributions of the  $^{16}\text{O}(^{12}\text{C},^{10}\text{B})^{18}\text{F}$  stripping reaction. The curves are EFR-DWBA fits. The normalization factors (experiment/theory) are 1.39, 0.27, 2.67, and 0.12 for the 11.2 MeV  $5^+$ , 9.35 MeV ( $6^-$ ), 10.23 MeV ( $4^-$ ), and 11.16 MeV ( $7^+$ ) states, respectively. The latter assignment corresponds to a tabulated level (Ref. 28).

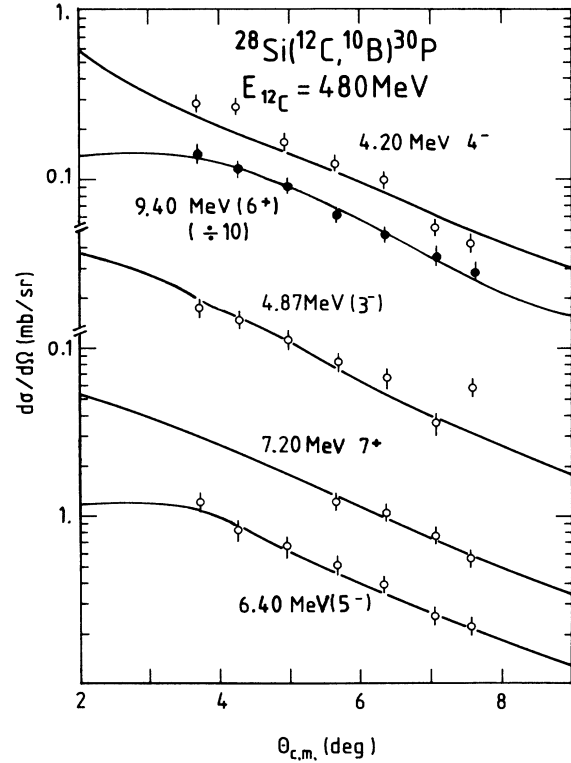


FIG. 11. Angular distributions of the  $^{28}\text{Si}(^{12}\text{C},^{10}\text{B})^{30}\text{P}$  deuteron stripping reaction. The solid curves are EFR-DWBA fits obtained with the optical model parameters given in Fig. 4. The normalization factors (experiment/theory) are 1.46, 2.88, 0.13, 0.19, and 1.27 for the 4.20 MeV  $4^-$ , 4.87 MeV ( $3^-$ ), 6.40 MeV ( $5^-$ ), 7.20 MeV  $7^+$ , and 9.40 MeV ( $6^+$ ) states, respectively.

Since a 4.92 MeV  $3^-$  level is tabulated<sup>20</sup> and an  $L_T=5$  transfer to a 6.50 MeV state is observed in the  $(\alpha,d)$  reaction,<sup>27</sup> a ( $5^-$ ) assignment is proposed for the 6.40 MeV state. The 9.40 MeV level seems to be linked to the second  $6^+$  states observed in  $^{30}\text{S}$  and  $^{30}\text{Si}$  (see Fig. 4), but no configuration may be proposed only on the basis of the present experiment.

Figure 11 presents the  $^{28}\text{Si}(^{12}\text{C},^{10}\text{B})^{30}\text{P}$  angular distributions for several excited levels of the  $^{30}\text{P}$  residual nucleus. The optical model parameters used<sup>18</sup> are those given in Fig. 5. The EFR-DWBA fits are quite good, but again the angular distributions have a shape rather independent of the final spin.

### C. $^3\text{He}$ stripping reactions

#### 1. $^{12}\text{C}(^{12}\text{C},^9\text{Be})^{15}\text{O}$

Figure 12 presents the  $^{12}\text{C}(^{12}\text{C},^9\text{Be})^{15}\text{O}$  spectrum measured at 480 MeV. This spectrum has to be compared with those obtained for the same reaction at much lower incident energies: 72, 114, and 174 MeV,<sup>1</sup> and at 240 MeV.<sup>30</sup> The 12.83 and 15.05 MeV levels were already strongly excited in the 114, 174, and 240 MeV  $^{12}\text{C}$  induced spectra, and were related to the following

stretched configurations  $((1d_{5/2})^2 1p_{1/2})_{11/2^-}$  and  $(1d_{5/2})^3_{13/2^+}$ . The location of this  $\frac{13}{2}^+$  configuration can be calculated from Eq. (4) using the experimental TBME deduced from two-nucleon-transfer reaction data of the present study and of others.<sup>3,4,25</sup> The resulting value 15.8 MeV is in good agreement with the observed experimental 15.05 MeV.

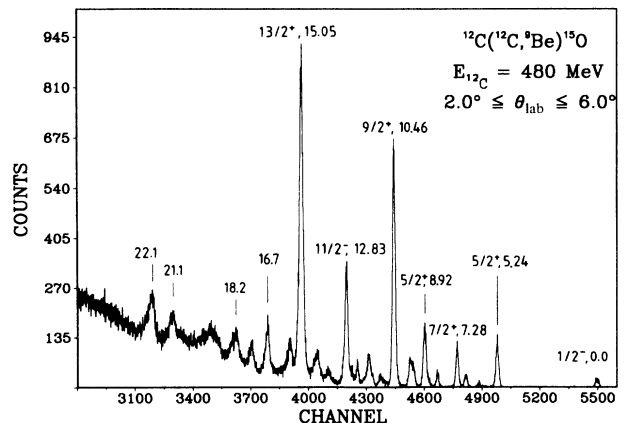


FIG. 12. The  $^{12}\text{C}(^{12}\text{C},^9\text{Be})^{15}\text{O}$   $^3\text{He}$ -stripping reaction.

The 10.46 MeV level, was also observed in the 114 and 240 MeV measurements, but was weakly excited. A tentative  $\frac{9}{2}^+$  spin parity assignment was made to this level.<sup>1,31</sup> One can use the following argument to explain that this state, having a lower spin than the 12.83 and the 15.05 MeV states, is excited as strongly, as those only at very high incident energy. Two  $\frac{9}{2}^+$  states have been calculated by Lie *et al.*<sup>32</sup> in a weak coupling approach. They consider particles (*p*) outside an  $^{16}\text{O}$  core and holes (*h*) in the *p* shell. Their first  $\frac{9}{2}^+$  state is predicted at 9.94 MeV with a main configuration  $(p_{9/2}^3 + (h)_{0+}^4)$  which can be compared with the  $(sd)_{9/2}^3$  configuration of the cluster model.<sup>1</sup> The second  $\frac{9}{2}^+$ , predicted at 11.45 MeV, contains an important  $(p)_{5/2}^1 + (h)_{2+}^2$  component, which implies at least one hole in a  $^{12}\text{C}$  core. Supposing that the 10.46 MeV level corresponds to this second  $\frac{9}{2}^+$  state would then explain why it is strongly populated at high bombarding energy only, likewise the  $2^+$  6.59 MeV state of the  $^{14}\text{O}$  nucleus produced in the two-proton stripping reaction (see Sec. IV A). At the energy of the present experiment, the two-step process necessary to populate such a configuration may occur and be of importance.

The experimental angular distributions of the most strongly populated states are presented in Fig. 13, along with EFR-DWBA curves, calculated on the assumption of a one-step  $^3\text{He}$  transfer. The optical model parameters used and given in the figure fit best the 420 MeV elastic scattering of  $^{12}\text{C}$  on  $^{12}\text{C}$ .<sup>18</sup>

## 2. $^{16}\text{O}(^{12}\text{C}, ^9\text{Be})^{19}\text{Ne}$

Figure 14 presents the  $(^{12}\text{C}, ^9\text{Be}) ^3\text{He}$  stripping obtained with a  $\text{SiO}_2$  target at 480 MeV. The g.s., 0.2 MeV doublet and 1.5 MeV multiplet are weakly populated. On the other hand, the 2.8 MeV  $\frac{9}{2}^+$  and 4.64 MeV  $\frac{13}{2}^+$  high spin states<sup>33</sup> are strongly populated. These two levels, and their analogs in  $^{19}\text{F}$ , were also strongly excited in the  $^{16}\text{O}(^6\text{Li}, t)^{19}\text{Ne}$  and  $^{16}\text{O}(^6\text{Li}, ^3\text{He})^{19}\text{F}$  reactions studied by Martz *et al.*<sup>34</sup> at 46 MeV, and in the  $^{16}\text{O}(^{10}\text{B}, ^7\text{Li})^{19}\text{Ne}$  and  $^{16}\text{O}(^{10}\text{B}, ^7\text{Be})^{19}\text{F}$  reactions studied by Hamm *et al.*<sup>35</sup> at 100 MeV, but not in  $\alpha$ -particle transfer<sup>34</sup> on  $^{15}\text{N}$ . So these two states belong to the  $(sd)^3, 2N+L$ , g.s. band and could have the following stretched configurations:  $((1d_{5/2})^2 2s_{1/2})_{9/2+}$  and  $(1d_{5/2})^3_{13/2+}$ , which are predicted at 3.8 and 4.9 MeV, respectively, from Eq. (4) using the experimental TBME deduced in the present work.

The 8.9 MeV level in  $^{19}\text{Ne}$  most probably corresponds to the 8.95 MeV  $^{19}\text{F}$  state, while the large peak observed at 9.8 MeV could be related to the 9.88 and 10.41 MeV  $^{19}\text{F}$  states, as it can be deduced from the comparison of spectra obtained with heavy ion<sup>34,35</sup> or  $\alpha$ -particle<sup>36,37</sup> induced analog reactions. From DWBA fits in an  $(\alpha, p)$   $^3\text{H}$ -transfer experiment,<sup>36</sup> spin parities of  $\frac{11}{2}^-$ ,  $\frac{11}{2}^+$ , and  $\frac{13}{2}^+$  have been inferred for these levels, assignments which were confirmed by  $(\alpha, \gamma)$  measurements,<sup>38</sup> except that the parity of the 9.88 MeV state was found to be negative.

The 12.3 MeV level in  $^{19}\text{Ne}$  is strongly populated as is its analog state in  $^{19}\text{F}$  at 12.7 MeV in the reactions men-

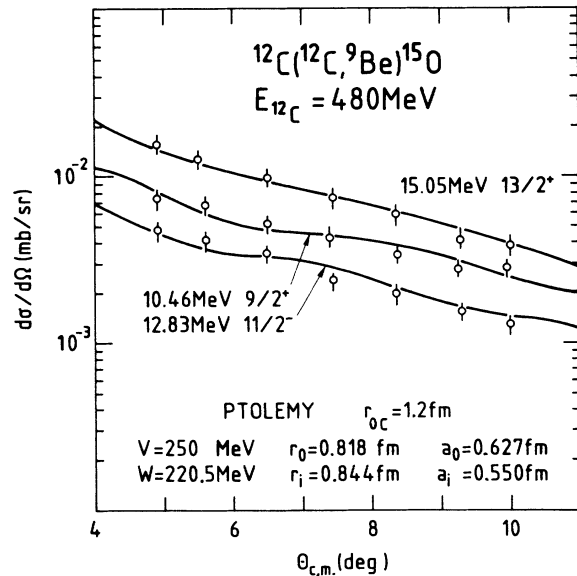


FIG. 13. Angular distributions of the  $^{12}\text{C}(^{12}\text{C}, ^9\text{Be})^{15}\text{O}$   $^3\text{He}$ -stripping reaction with the corresponding EFR-DWBA fits. The values of the normalization factor (experiment/theory) are 0.027, 0.064, and 0.022 for the 10.46 MeV  $\frac{9}{2}^+$ , 12.83 MeV  $\frac{11}{2}^-$ , and 15.05 MeV  $\frac{13}{2}^+$  states, respectively.

tioned above.<sup>34-36</sup> A  $\frac{15}{2}^-$  spin parity is proposed for the 12.7 MeV state, on the basis of an  $\alpha$ -particle stripping study done by Pilt *et al.*<sup>39</sup> in the  $^{15}\text{N}(^{13}\text{C}, ^9\text{Be})^{19}\text{F}$  reaction. A  $((1d_{5/2})^2_{5+} + 1f_{7/2})_{17/2-}$  stretched configuration for the 12.3 MeV level would explain its strong population in the present transfer reaction.

Figure 15 presents the angular distributions of the  $^{16}\text{O}(^{12}\text{C}, ^9\text{Be})^{19}\text{Ne}$  stripping reaction for several states. The EFR-DWBA fits are rather good but spin independent. The optical model parameters<sup>18</sup> are those of a  $^{12}\text{C}$  target and are given in Fig. 13. The overall normaliza-

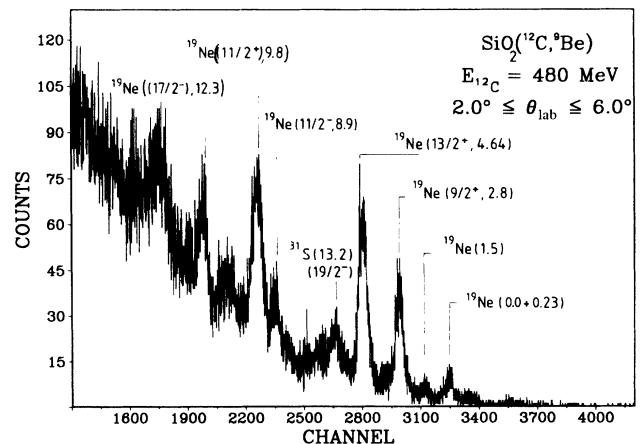


FIG. 14. The energy spectrum of the  $(^{12}\text{C}, ^9\text{Be}) ^3\text{He}$ -stripping reactions obtained with a  $\text{SiO}_2$  target.

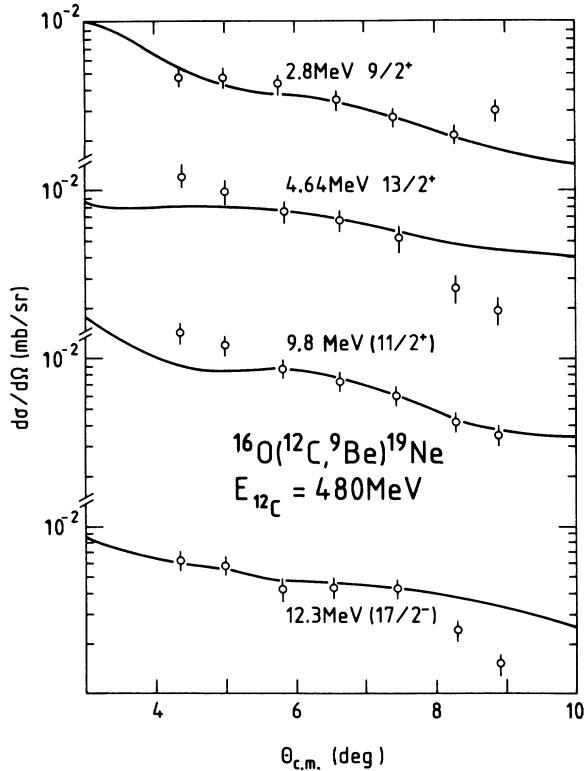


FIG. 15. Angular distributions of the  $^{16}\text{O}(^{12}\text{C}, ^9\text{Be})^{19}\text{Ne}$   $^3\text{He}$ -stripping reaction. The solid curves are EFR-DWBA fits obtained with the optical model parameters given in Fig. 13. The normalization factors (experiment/theory) are 0.039, 0.043, 0.105, and 0.001 for the 2.8 MeV  $\frac{9}{2}^+$ , 4.64 MeV  $\frac{13}{2}^+$ , 9.8 MeV ( $\frac{11}{2}^+$ ), and 12.3 MeV ( $\frac{17}{2}^-$ ) states, respectively.

tion factors reported in the figure caption can be compared with the relative spectroscopic factors for three-nucleon clusters in  $^{19}\text{F}$  and  $^{19}\text{Ne}$ , taken from experimental  $^3\text{He}$  transfer reaction data and from shell model calculations.<sup>40</sup> The relative spectroscopic factor obtained for the  $\frac{13}{2}^+$  4.6 MeV  $^{19}\text{Ne}$  state is in agreement with the value reported for its analog, contrary to the result obtained at lower incident energy.<sup>38,40</sup>

### 3. $^{28}\text{Si}(^{12}\text{C}, ^9\text{Be})^{31}\text{S}$

In the spectrum of Fig. 14, one peak has been attributed on focalization considerations to an unknown state in  $^{31}\text{S}$ . Its excitation energy of 13.2 MeV is consistent with the value 12.3 MeV calculated from Eq. (4) for a  $(1f_{7/2})^3_{19/2-}$  configuration with single particle energies of Refs. 20 and 41 (Table I).

### 4. $^{40}\text{Ca}(^{12}\text{C}, ^9\text{Be})^{43}\text{Ti}$

The only strongly populated state in the  $^{40}\text{Ca}(^{12}\text{C}, ^9\text{Be})^{43}\text{Ti}$  reaction is the  $\frac{19}{2}^-$  3.066 MeV state,<sup>42</sup> already observed at lower incident energy.<sup>1</sup> Its cross section is  $1 \mu\text{b}/\text{sr}$  at  $5.0^\circ$  (c.m.). The configuration of this state is  $(1f_{7/2})^3_{19/2-}$  and its calculated excitation energy is 3.13 MeV from Eq. (4) and the present experimental TBME.

### V. CONCLUSION

Multinucleon transfer reactions induced by  $^{12}\text{C}$  at 40 MeV/u still populate strongly and selectively high spin states. In the case of reactions transferring a pair of nucleons, the near correspondence of the crude shell model estimates of excitation energies for stretched spin configurations and observed states allows possible spin assignments in a very simple way. Experimental two-body matrix elements can be obtained from states known to have rather pure two-nucleon configurations and they can then be used to characterize states of three-nucleon configurations. Unfortunately, the angular distributions of these heavy ion reactions are rather independent of the final state spin. Contrary to the case of one-nucleon stripping reactions, the usual treatment of multinucleon transfer reactions requires tedious shell model spectroscopic factor computations and the  $0s$  cluster approximation can be too drastic because of neglect of higher-order terms. On the other hand, the high bombarding energy in the present work favors processes less simple than one-step direct stripping, and gives some unexpectedly interesting results concerning the strong excitation of hole states (e.g., the  $2^+$  state at 6.59 MeV in  $^{14}\text{O}$ ) and two-particle transfer on a polarized target (the second  $6^+$  state at 9.9 MeV in  $^{30}\text{S}$ ).

### ACKNOWLEDGMENTS

It is a pleasure to acknowledge very enlightening discussions with Dr. Tsan Ung Chan, Professor A. Poves, and Dr. A. Zuker. We wish to thank Dr. D. Disdier and Dr. A. Abzouzi for their efficient help and Dr. A. Pape for a rigorous and critical reading of this article. Sincere thanks are also due to Mrs. J. Sauret and the operating staff of the GANIL cyclotrons for the excellent quality of the  $^{12}\text{C}$  beam. The stay in France of one of us (A.M.) has been supported by the Deutsche Forschungsgemeinschaft.

<sup>1</sup>N. Anyas-Weiss, J. C. Cornell, P. S. Fisher, P. N. Hudson, A. Menchaca-Rocha, D. J. Millener, A. D. Panagiotou, D. K. Scott, D. Strottman, D. M. Brink, B. Buck, P. J. Ellis, and T. Engeland, *Phys. Rep.* **12C**, 201 (1974).

<sup>2</sup>H. Homeyer, F. D. Becchetti, B. G. Harvey, D. L. Hendrie, D. G. Kovar, J. Mahoney, and W. von Oertzen, Lawrence

Berkeley Laboratory Report No. LBL-4000, 67, 1975 (unpublished).

<sup>3</sup>E. Rivet, R. H. Pehl, J. Cerny, and B. G. Harvey, *Phys. Rev.* **141**, 1021 (1966); C. C. Lu, M. S. Zisman, and B. G. Harvey, *Phys. Rev. C* **186**, 1086 (1969).

<sup>4</sup>R. Jahn, G. J. Wozniak, D. P. Stahel, and J. Cerny, *Phys. Rev.*

- Lett. **37**, 812 (1976); R. Jahn, D. P. Stahel, G. J. Wozniak, R. J. de Meijer, and J. Cerny, Phys. Rev. C **18**, 9 (1978).
- <sup>5</sup>R. J. de Meijer, R. Kamermans, J. Van Driel, and M. P. Morsch, Phys. Rev. C **16**, 2442 (1977); J. Van Driel, R. Kamermans and R. J. de Meijer, Nucl. Phys. **A350**, 109 (1980).
- <sup>6</sup>Tsan Ung Chan, Phys. Rev. C **36**, 838 (1987); Tsan Ung Chan, M. Agard, J. F. Bruandet, and C. Morand, *ibid.* **19**, 244 (1979).
- <sup>7</sup>P. Birien and S. Valero, CEN Saclay Note No. CEA-N-2215 (1981); J. Gastebois, *Detectors in Heavy Ion Reactions*, Vol. 178 of *Lecture Notes in Physics*, (Springer, Berlin, 1983), p. 126.
- <sup>8</sup>P. J. Brussaard and P. W. M. Glaudemans, *Shell Model Applications in Nuclear Spectroscopy* (North-Holland, Amsterdam, 1977), p. 41.
- <sup>9</sup>G. Audi and A. Wapstra, The 1986 Audi-Wapstra MID-stream Mass evaluations, distributed by P. Haustein (Brookhaven National Laboratories, 1986).
- <sup>10</sup>B. Buck, in *Nuclear Spectroscopy and Nuclear Reactions with Heavy Ions*, Proceedings of the International School of Physics "Enrico Fermi," course LXII, edited by H. Faraggi and R. A. Ricci (North-Holland, Amsterdam, 1976), p. 29; D. Kurath, *ibid.*, p. 58.
- <sup>11</sup>M. H. Macfarlane and S. C. Pieper, Argonne National Laboratory Report No. ANL-76-11 Rev. 1, Mathematics and Computers, UC 32 (1976).
- <sup>12</sup>M. Hamm and K. Nagatani, Phys. Rev. C **17**, 586 (1978).
- <sup>13</sup>D. K. Scott, D. L. Hendrie, U. Jahnke, L. Kraus, C. F. Maguire, J. Mahoney, Y. Terrien and K. Yagi, Lawrence Berkeley Laboratory Report No. LBL-4000, 77 (1975); H. G. Bohlen, L. Kraus, I. Linck, A. Miczaika, R. Rebmeister, N. Schulz, and W. Weller, Centre de Recherche Nucléaires, Strasbourg, Rapport-d'activité 1984, (unpublished).
- <sup>14</sup>M. B. Greenfield, C. R. Bingham, E. Newman, and M. J. Saltmarsh, Phys. Rev. C **6**, 1756 (1972).
- <sup>15</sup>S. Lie, Nucl. Phys. **A181**, 517 (1982).
- <sup>16</sup>J. G. Pronko, R. G. Hirko, and D. C. Slater, Phys. Rev. C **7**, 1382 (1973).
- <sup>17</sup>R. J. Peterson and J. J. Hamill, Phys. Rev. C **22**, 2282 (1980).
- <sup>18</sup>C.-C. Sahn, T. Murakami, J. G. Cramer, A. J. Lazzarini, D. D. Leach, D. R. Tieger, R. A. Loveman, W. G. Lynch, M. B. Tsang, and J. Van der Plicht, Phys. Rev. C **34**, 2165 (1986).
- <sup>19</sup>H. T. Fortune, L. C. Bland, and W. D. M. Rae, J. Phys. G. **11**, 1175 (1985).
- <sup>20</sup>P. M. Endt and C. Van der Leun, Nucl. Phys. **A310**, 1 (1978).
- <sup>21</sup>D. Evers, W. Assmann, K. Rudolph, S. J. Skorka, and P. Sperr, Nucl. Phys. **A230**, 109 (1974).
- <sup>22</sup>W. P. Alford, R. A. Lindgren, D. Elmore, and R. N. Boyd, Phys. Rev. C **10**, 1013 (1971).
- <sup>23</sup>W. Bohne, K. D. Büchs, H. Fuchs, K. Grabisch, D. Hilscher, U. Janetzki, U. Jahnke, H. Kluge, T. G. Materson, and H. Morgenstern, Nucl. Phys. **A284**, 14 (1971).
- <sup>24</sup>Huo Junde, Hu Dailing, Zhou Chunmei, Han Xiaoling, Hu Baohua, and Wu Yaodong, Nuclear Data Sheets **51**, 1 (1987).
- <sup>25</sup>R. Jahn, U. Wienands, D. Wenzel, and P. von Neumann-Cosel, Phys. Lett. **150B**, 331 (1985).
- <sup>26</sup>J. K. Tuli, R. R. Kinsey, and M. J. Martin, Nuclear Data Sheets **44**, 3 (1985).
- <sup>27</sup>Y. Kadota, K. Ogino, K. Obori, Y. Taniguchi, T. Tanabe, M. Yasue, and J. Schmizu, Nucl. Phys. **A458**, 523 (1986).
- <sup>28</sup>F. Ajzenberg-Selove, Nucl. Phys. **A300**, 1 (1978); **A360**, 1 (1981); **A460**, 1 (1986).
- <sup>29</sup>X. Campi, H. Flocard, A. K. Kerman, and S. Koonin, Nucl. Phys. A **251**, 193 (1975); A. Watt, R. P. Singhal, M. H. Storm, and R. R. Whitehead, J. Phys. G **7**, L145 (1981); M. H. Storm,, A. Watt, and R. R. Whitehead, *ibid.* **9**, L165 (1983); A. Cortès, thèse d'état, Université Louis Pasteur, Strasbourg (1983).
- <sup>30</sup>H. G. Bohlen, L. Kraus, I. Linck, A. Miczaika, R. Rebmeister, N. Schulz, and W. Weller, Centre de Recherches Nucléaires, Strasbourg, Rapport-d'activité 1984, (unpublished); H. G. Bohlen, B. Gebauer, L. Kraus, I. Linck, A. Miczaika, W. von Oertzen, R. Rebmeister, N. Schulz, W. Weller, and T. Wilpert Progress Report of the Hahn Reiter Institute, Berlin, 1986 (unpublished).
- <sup>31</sup>H. M. Kuan, D. G. Shirk, and S. Fiarman, Phys. Rev. C **15**, 569 (1977).
- <sup>32</sup>S. Lie, T. Engeland, and G. Dahll, Nucl. Phys. **A156**, 449 (1970); S. Lie and T. Engeland, *ibid.* **267**, 123 (1976).
- <sup>33</sup>F. Ajzenberg-Selove, Nucl. Phys. **A392**, 1 (1983).
- <sup>34</sup>L. M. Martz, S. J. Sanders, P. D. Parker, and C. B. Dover, Phys. Rev. C **20**, 1340 (1979).
- <sup>35</sup>H. Hamm, C. W. Towsley, R. Hanus, K. G. Nair, and K. Nagatani, Phys. Rev. Lett. **36**, 846 (1976).
- <sup>36</sup>K. Van der Borg, R. J. de Meijer, and A. Van der Woude, Nucl. Phys. **A273**, 172 (1976).
- <sup>37</sup>D. J. Overway and W. C. Parkinson, Nucl. Phys. **A363**, 93 (1981).
- <sup>38</sup>T. J. M. Symons, L. K. Fifield, M. J. Hurst, A. Pakkanen, F. Watt, C. H. Zimmerman, and K. W. Allen, Phys. Lett. **63B**, 409 (1976); L. K. Fifield, T. J. M. Symons, C. H. Zimmerman, M. J. Hurst, F. Watt, and K. W. Allen, *ibid.* **68B**, 125 (1977).
- <sup>39</sup>A. A. Pilt, D. J. Millener, H. Bradlow, O. Dietzsch, P. S. Fisher, W. J. Naude, W. D. M. Rae, and D. Sinclair, Nucl. Phys. **A273**, 189 (1976).
- <sup>40</sup>N. S. Godwin, W. D. M. Rae, B. Cooke, A. Etchegoyen, N. J. Eyre, P. S. Fisher, G. Proudfoot, and D. Sinclair, Nucl. Phys. **A363**, 493 (1981).
- <sup>41</sup>R. J. Peterson, C. A. Fields, R. S. Raymond, J. R. Thiele, and J. L. Ullman, Nucl. Phys. **A408**, 221 (1983).
- <sup>42</sup>L. Meyer-Schützmeister, A. J. Elwyn, S. A. Gronemeyer, G. Hardie, R. E. Holland, and K. E. Rehm, Phys. Rev. C **18**, 1148 (1978).